



Supported dual-acidic 1,3-disulfoimidazolium chlorozincate@HZSM-5 as a promising heterogeneous catalyst for synthesis of indole derivatives

Susmita Saikia | Krishna Puri | Ruli Borah

Department of Chemical Sciences, Tezpur University, Napaam, Tezpur 784028, India

CorrespondenceRuli Borah, Department of Chemical Sciences, Tezpur University, Napaam, Tezpur 784028, India.
Email: ruli@tezu.ernet.in**Funding information**

SERB-DST India, Grant/Award Number: EMR/2016/002108

HZSM-5-supported Brønsted and Lewis acidic ionic solid 1,3-disulfoimidazolium chlorozincate materials ($[\text{dsim}]_2[\text{ZnCl}_4]@\text{HZSM-5}$) were synthesized with various ratios (3, 6, 9, 17 and 50% w/w). The heterogeneous materials were characterized via a variety of spectroscopic techniques. Dual acidity of these materials was determined using specified techniques. These acidic solids were examined as stable heterogeneous catalysts for the Fischer indole reaction of equimolar amounts of phenylhydrazine hydrochloride and various aliphatic or aromatic ketones at 80–90°C in neat condition to produce substituted indole derivatives. The efficient 17% ionic salt-loaded HZSM-5 composite was easily reused for ten consecutive cycles with a slight loss of its activity. The recycled catalyst was further analysed using powder X-ray diffraction and inductively coupled plasma optical emission spectrometric techniques.

KEYWORDS

1,3-disulfoimidazolium chlorozincate, Brønsted–Lewis acidic, HZSM-5-supported ionic salt, indoles, reusable catalyst

1 | INTRODUCTION

The growing importance of supports in research fields has attracted attention towards zeolite materials for their ubiquitous influence as acidic, porous, crystalline, high-surface-area materials. Combining the characteristics of zeolite with target-specific solid or liquid catalysts via immobilization often results surface-modified stable reactive heterogeneous catalytic systems with high surface area. The selection of siliceous ZSM-5 as support among various types of zeolites is considered in terms of its unique shape selectivity, solid acidity, ion exchangeability, pore size, thermal stability and structural network.^[1] The presence of medium pore size (5.1–5.6 Å) bearing three-dimensional channels defined by 10-membered rings and smaller crystallite sizes of ZSM-5 framework can work as better support for immobilization of active catalytic species on its surface.^[2,3] Furthermore, high

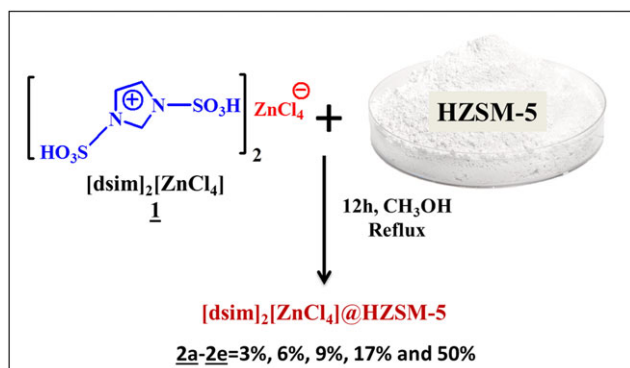
Si/Al ratio of the ZSM-5 support prevents de-alumination of framework Al which is a common problem of many other zeolites used as supports for immobilization of acidic materials. Nowadays, immobilization of catalytically active metals and nanomaterials onto heterogeneous supports is very common.^[4–7] Large numbers of zeolite-supported catalytic systems have been developed for utilization as efficient heterogeneous catalysts in organic synthesis.^[8,9] Most of these catalysts include reactive metal, their salts, oxide, metal complexes, nanomaterials, etc.^[10–13]

There are only a few reports of the design and uses of ionic liquid/solid supported zeolite composites as heterogeneous catalysts.^[14–17] The concept of an ‘ionic liquid’ is an area beyond the scope of the present paper.^[18] Amidst the numerous members of the ionic liquid family, some of them have extended their use from homogeneous room temperature liquids to heterogeneous solids. Inclusion of

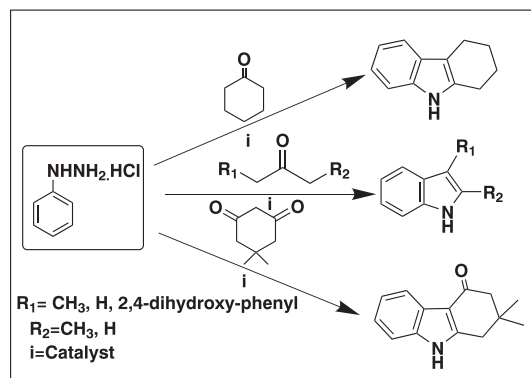
complex metal halide anions with organic cations generates solid or semisolid-like materials. Transition metal halides have been utilized as anionic counterparts of an ionic liquid-based system which has been defined as 'chlorometallate' as one important class of functionalized ionic solid. Structural variations of cationic and anionic counterparts of ionic liquids mainly contribute the specific behavioural differences depending on the functionalities present. Most of them are hygroscopic solids (or semisolids) with low thermal stability which reduces their lifetime although they have excellent Brønsted–Lewis acidic natures.^[19] The water sensitivity of these materials can be improved after being loaded on the surface of ZSM-5 zeolite in various compositions. There is a possibility for increasing the thermal stability of composites with modification of catalytic sites of the acidic ionic material on the surface of a support. This process can be utilized to combine certain specific features of metal-containing ionic solids (e.g. Brønsted–Lewis acidity, magnetic properties, fluorescence, etc.) with unique properties of a zeolite support for efficient applications as solid acidic composites.^[20] In this context, we aimed to immobilize a known^[19] Brønsted–Lewis acidic 1,3-disulfoimidazolium chlorozincate ($[\text{dsim}]_2[\text{ZnCl}_4]$) ionic salt on HZSM-5 support with various ratios (3, 6, 9, 17 and 50% w/w) for the formation of stable composites by a wet impregnation method (Scheme 1).^[21]

The prepared composites were characterized using various analytical techniques to understand their thermal stability, acidic strength, surface morphology and Brunauer–Emmett–Teller (BET) surface area and also the interaction of the ionic salt with the zeolite support. Finally they were examined as possible reusable supported acid catalysts for the Fischer indole reaction (Scheme 2) in solvent-free medium.

The potential of the Fischer indole reaction has been observed with stoichiometric amounts of a variety of Brønsted or Lewis acid catalysts (e.g. H_2SO_4 , HCl , polyphosphoric acid, ZnCl_2 , FeCl_3 , AlCl_3 , etc.) and also with other solid acids.^[22–26] These catalytic systems



SCHEME 1 Synthesis of $[\text{dsim}]_2[\text{ZnCl}_4]@\text{HZSM-5}$



SCHEME 2 Fischer indole reaction

suffer from considerable drawbacks such as low yield, harsh or delicate reaction condition, by-products, high temperatures, prolonged reaction times and tedious work-up procedures. Few catalytic systems have been introduced for the Fischer indole reaction involving ionic liquid as reaction medium with added Lewis acid catalyst or use of task-specific acidic ionic liquids to work as dual solvent–catalysts in solution or solvent-free medium at various temperatures.^[27–29] Indole and its derivatives constitute a major class of N-heterocycles in various biochemical processes as they are a part of some essential amino acids and most proteins. Many of them act as anticancer, antileukemic, antidepressant, antihypertensive, immune modulating agents, etc.^[30,31] Vincristine is a drug molecule of clinical interest possessing antitumour activities.^[30] The initial Lewis acidic ionic liquid catalyst 1-butyl-pyridinium chloride· 3AlCl_3 worked as dual solvent–catalyst for the Fischer indole reaction with excellent catalytic activity.^[32] Ionic liquid choline chloride· 2ZnCl_2 was also successfully used as solvent–catalyst for this reaction.^[33] In spite of the robust catalytic activities of such Lewis acidic ionic liquids, they were not recycled because of their air- and moisture-sensitive nature. Catalytic recyclable Brønsted acidic imidazolium ionic liquids functionalized with two alkyl sulfonic acid groups were designed by Xu *et al.* for the Fischer indole reaction in water at $80\text{--}100^\circ\text{C}$ for 0.5–6 h reaction time.^[34] Neuhaus and co-workers also conducted the Fischer indole synthesis of wide variety of hydrazine and ketones in the presence of the acidic ionic liquid tetramethylguanidinium propanesulfonic acid trifluoromethyl acetate in water at 90°C .^[27] In 2012, Li *et al.* designed a series of $-\text{SO}_3\text{H}$ -functionalized imidazolium ionic liquids and employed them as reusable catalysts for one-pot Fischer indole synthesis under microwave irradiation in water.^[35] An ultrasound-assisted route for the same synthesis was introduced by Tao *et al.* in water in the presence of imidazolium ionic liquid bearing two alkyl sulfonic acid groups at 100°C

within a short reaction time.^[36] The literature also reveals one example of a silica-supported $-\text{SO}_3\text{H}$ -bearing acidic ionic liquid as a heterogeneous catalyst for the reaction of phenylhydrazines with ketones or aldehydes at room temperature.^[37]

2 | EXPERIMENTAL

2.1 | Catalyst characterization

A Nicolet Impact-410 spectrophotometer was used for recording Fourier transform infrared (FT-IR) spectra. Thermogravimetric analysis (TGA) was done with a Shimadzu TGA-50. The Brønsted acidities of the supported composites were obtained with a UV 2550 spectrophotometer using 4-nitroaniline as basic indicator. Scanning electron microscopy (SEM) images were obtained with a JEOL JSM-6390LVSEM, equipped with energy-dispersive X-ray (EDX) analyser. Raman spectra of the composites were obtained using a Renishaw spectrophotometer equipped with a He-Ne laser of excitation wavelength 514 nm. BET isotherms were recorded with a Quantachrome NOVA 1000E surface pore size analyser. Powder X-ray diffraction (PXRD) patterns were recorded with a Rigaku Multiflex instrument using a nickel-filtered Cu K (0.15418 nm) radiation source and scintillation counter detector. UV-visible diffuse reflectance spectra were obtained using a Shimadzu UV 2450 spectrophotometer. Melting points were determined with a Buchi-560 melting point apparatus. The ^1H NMR and ^{13}C NMR spectra of the indole derivatives were obtained with a JEOL 400 MHz spectrophotometer with CDCl_3 as solvent. Inductively coupled plasma optical emission spectrometry (ICP-OES) was conducted with a PerkinElmer Optima 2100DV instrument.

2.2 | Preparation of $[\text{dsim}]_2[\text{ZnCl}_4]$ @HZSM-5

The ammoniated ZSM-5 powders ($\text{Si}/\text{Al} = 80$) and all other chemicals used in this study were purchased from Acros Chemicals. The ionic chlorometallate was synthesized according to a reported method.^[18] Then ZSM-5 powder was calcined in a muffle furnace at $550\text{--}600^\circ\text{C}$ to afford the final degassed sample as HZSM-5. After calcining, HZSM-5 powder was treated with pre-synthesized 1,3-disulfoimidazolium chlorozincate (**1**) with various ratios (3, 6, 9, 17 and 50% w/w) in methanol at 80°C for 12 h (Scheme 1). The resultant supported materials were collected after evaporation of methanol in a rotary evaporator and were dried again in a vacuum oven at 100°C .

2.3 | Catalytic investigation

A typical reaction of phenylhydrazine hydrochloride (1 mmol) with ketone (or aldehyde) (1 mmol) using a catalytic amount (10 mg) of $[\text{dsim}]_2[\text{ZnCl}_4]$ @HZSM-5 was performed at $80\text{--}100^\circ\text{C}$ under neat condition for a specific reaction time to afford the respective indole derivatives. Product formation was monitored by TLC using 1:5 EtOAc-hexane as mobile phase. After that the reaction mixture was cooled immediately to room temperature and the organic mixture extracted with dichloromethane (DCM). The catalyst was insoluble in DCM. Thus decantation of DCM with further washing several times using the same solvent gave the recycled catalyst. Then the organic phase was dried over Na_2SO_4 and the solvent was removed in a rotary evaporator. Recrystallization from ethanol and water gave the desired solid product in satisfactory yield. This process was repeated two to three times to obtain analytically pure product.

3 | RESULTS AND DISCUSSION

At first, the synthesis of five $[\text{dsim}]_2[\text{ZnCl}_4]$ @HZSM-5 composite materials was conducted after impregnation of $[\text{dsim}]_2[\text{ZnCl}_4]$ ionic salt with ratios of 3, 6, 9, 17 and 50% (w/w) on HZSM-5 support according to Scheme 1. Then these five samples were subjected to various analytical techniques which included FT-IR spectroscopy, TGA, PXRD, Raman spectroscopy, SEM, EDX, Hammett acidity and Lewis acidity determination, electronic spectroscopy and BET analysis. These analyses gave valuable information about the physicochemical nature of the composites such as thermal stability, hygroscopic properties, Brønsted-Lewis acidities, surface area and also crystallinity of the HZSM-5 support. In the next step, we studied the possible uses of these composites as supported solid acid catalysts for the Fischer indole reactions of phenylhydrazine with a variety of carbonyl compounds in solvent-free medium at various temperatures.

3.1 | FT-IR study of **1**@HZSM-5

Various structural constituents and crystallinity related to their characteristic occupancy in the zeolite framework were primarily distinguished from FT-IR stretching and bending vibrations for the support HZSM-5 and hybrid samples of Zn^{2+} (**2a-2e**) (Figure 1; Table 1). Evidence for the existence of crystalline phases in all the modified materials was determined using the two absorptions at 543 and 450 cm^{-1} .^[38,39] The degree of

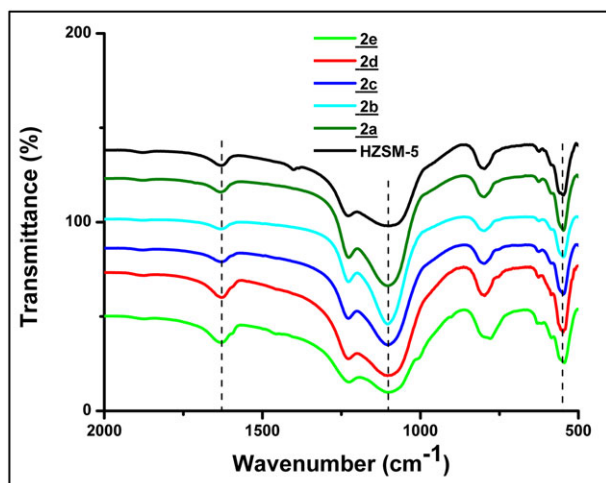


FIGURE 1 FT-IR spectra of **1**@HZSM-5 (**2a**–**2e**) and HZSM-5

TABLE 1 FT-IR peak assignments of **1**@HZSM-5

| Peak (cm ⁻¹) | Assignment |
|--------------------------|--|
| 450 | T–O bending vibrations of SiO ₄ and AlO ₄ internal tetrahedron |
| 543–553 | Double five-ring lattice vibration of external linkages |
| 797–801 | External symmetric vibrations of T–O–T linkage (T = Si or Al) |
| 1075 | Asymmetric stretching vibration of –SO ₃ H group overlapped with asymmetric T–O band |
| 1106–1230 | Internal asymmetric stretching vibrations of T–O–T linkage |
| 1630 | Bending vibration due to adsorbed water on HZSM-5 framework merged with C=N stretching vibration of imidazolium cation |

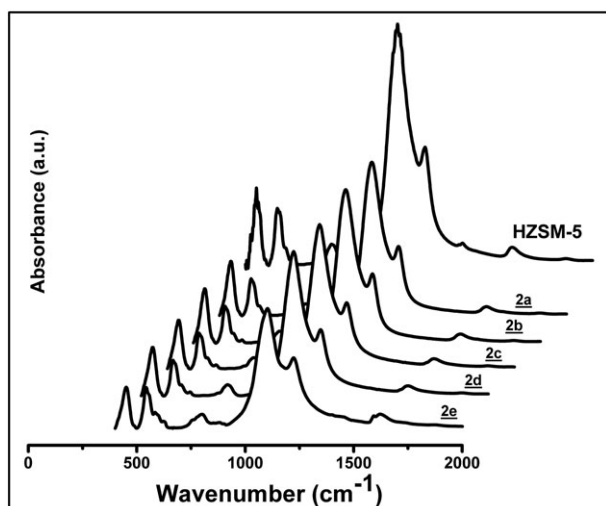


FIGURE 2 FT-IR absorption spectra of **1**@HZSM-5 (**2a**–**2e**)

crystallinity estimated from the ratio of the intensities of these two peaks (Table S1; Figure 2) was found to be in the range 0.78–0.82 which was in accordance with the reported value of 0.8 for pure HZSM-5.^[40,41] The crystallinity analysis along with the respective FT-IR spectra made a clear point about loss of some degree of crystallinity in the case of the 50% loaded material (Table S2; intensity ratio > 0.85) (**2e**) which was later confirmed by PXRD analysis. Also the FT-IR spectrum indicates the destruction of the framework by displaying additional peak at 1592 cm⁻¹ as well as some discrepancy around 797–801 cm⁻¹. We analysed the O–H stretching vibration of hybrid samples within the frequency range 3000–3800 cm⁻¹ (Figure 3). The reason behind this behaviour shown by the highest loaded composite can be accounted for by framework discontinuity due to possible insertion and reinsertion of Al atoms associated with the zeolite network. Reinsertion of EFAl (extraframework Al) species into the zeolite as framework Al is evidenced from the reduction of peak intensity at 3662 cm⁻¹ with increasing loading up to 17% of ionic salt in composite materials. The absorption maximum of hydroxyl peak at 3452 cm⁻¹ shifts towards 3610 cm⁻¹ as a broad band which can be reasoned as the presence of framework Al with increasing loading of the ionic salt.^[42] This type of acidic salt-mediated insertion of Al is supported by the work done by Fan *et al.*^[43] Alkali-mediated desilication of highly siliceous HZSM-5 structure with 50% loaded hybrid samples can be indicated by absorption in the range 2800–3200 cm⁻¹ which again may occur by *in situ* formation of metal hydroxide of Zn²⁺ from water-sensitive chlorometallates during the preparation of 50% loaded zeolite. Therefore, we have got comparable thermal stabilities of the 50% loaded sample (**2e**) with the bare ionic salt (**1**) in TGA (Figure 4).

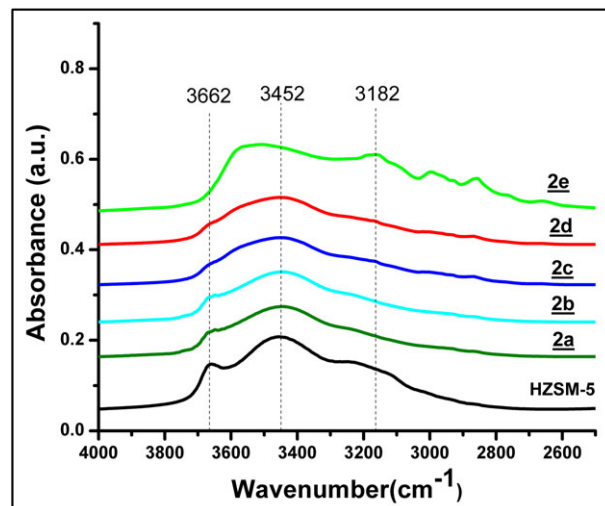


FIGURE 3 OH stretching vibration bands of **1**@HZSM-5 (**2a**–**2e**)

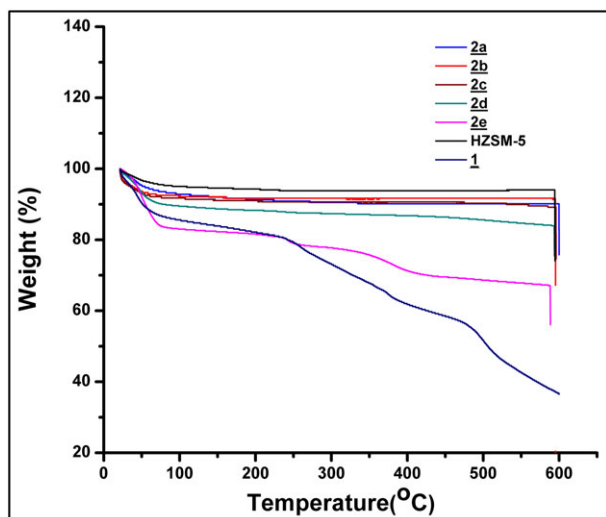


FIGURE 4 TGA curves of 1@HZSM-5 (2a–2e), HZSM-5 and 1a

3.2 | Thermogravimetric analysis

The TGA profiles displayed 3–8% weight loss below 100°C which may be attributed to the loss of absorbed moisture. Beyond this, the curves express high thermal stability in the case of 2a–2d (3–17%) up to 600°C, similar to that of parent HZSM-5. But 2e (50% loaded material) behaved more like the original ionic salt which is very hygroscopic as well.

3.3 | PXRD analysis

Figure 5 reveals identical patterns of PXRD peaks in the case of chlorometallate-loaded HZSM-5 hybrids 1@HZSM-5 (2a–2d) to that of the parent zeolite, except for 2e. The highest loaded material (50%, 2e) showed a

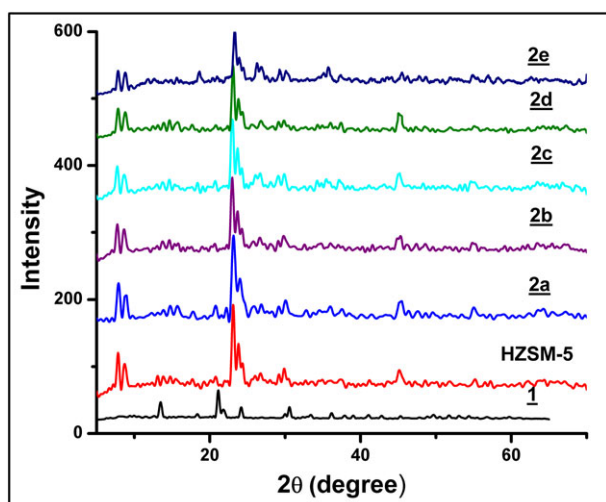


FIGURE 5 PXRD patterns of 1@HZSM-5 (2a–2e), HZSM-5 and 1

decrease in peak intensity at $2\theta = 7.78^\circ$, 23.07° and 45.1° .^[44,45] PXRD patterns strongly established the retention of crystallinity in synthesized materials 2a–2d without displaying any characteristic peak of the bare ionic salt. Figure 6 shows the degree of crystallinity of the loaded materials for the four intense peaks in the region $2\theta = 8\text{--}45^\circ$ with respect to HZSM-5. The values calculated from the graph indicate the gradual loss of crystallinity of the 1@HZSM-5 materials up to 17% loading. Sample 2e has lost maximum crystallinity due to its hydrophilic nature and thus destabilization results from the dissolution of the HZSM-5 framework evidenced from Figure 3 (O–H stretching) and Figure 4 (TGA profile).

3.4 | Raman spectra

Owing to the ambiguous behaviour of the highest loaded hybrid 2e, we chose to consider only 1@HZSM-5 materials up to 17% loading. Therefore, Raman spectra (Figure 7) were recorded for only the lowest (3%, 2a) and highest loaded materials (17%, 2d) with respect to the parent HZSM-5. Characteristic peaks showed evidence of respective hybrids with intactness of the MFI topology of HZSM-5. The symmetric stretching modes of Si–O–Si bonds of five-membered silicate frameworks of MFI unit structure in addition to other characteristics bands appeared at 290, 380 and 460 cm^{-1} .^[46] The basic peak of HZSM-5 at 298 cm^{-1} slightly changed its position to 300 and 295 cm^{-1} due to the presence of Zn^{2+} . The other important peak at 460 cm^{-1} is also shifted to some extent.

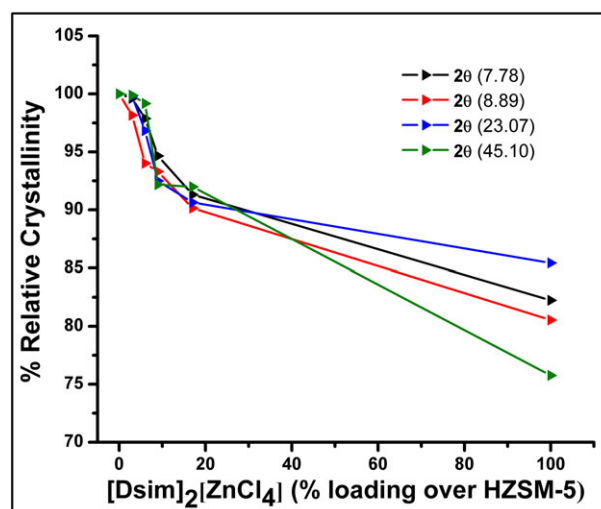


FIGURE 6 Crystallinity of 1@HZSM-5 (2a–2e) with respect to parent HZSM-5

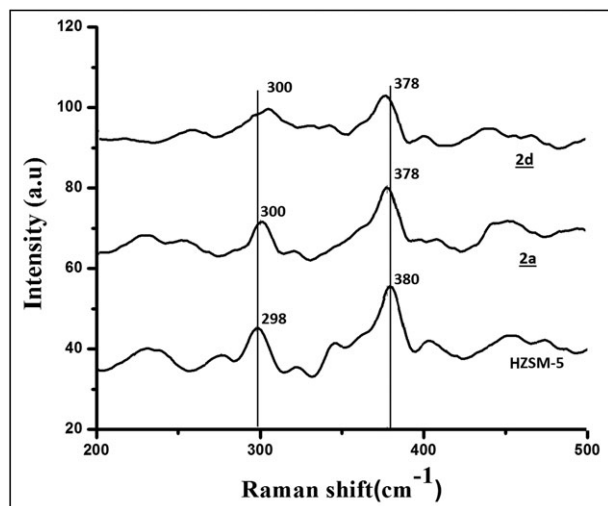


FIGURE 7 Raman spectra of **1@HZSM-5 (2a and 2d)** with respect to parent HZSM-5

3.5 | SEM and EDX analyses

Surface morphological changes and discrepancies resulting from loading of ionic salt **1** onto HZSM-5 can be assessed from SEM analyses of **2a** and **2d** along with HZSM-5 (Figure 8). Composite **2a** displayed a little aggregation on the surface with negligible change in crystalline phase while **2d** showed clogging of pores with some cluster formation due to expected hydrogen bonding occurring between Brönsted acidic sites of the ionic salt with framework Al generated from re-alumination of EFAl to the parent HZSM-5 as described in the study of O—H stretching vibrations (Figure 3). Likewise, the EDX analysis of **2d** confirmed the presence of Zn²⁺ along with Al, Si, Cl, N, O and S of the **1@HZSM-5** material.

3.6 | Hammett acidity determination using UV-visible spectrophotometry

We determined the trend in Brönsted acidity in loaded zeolite materials **1@HZSM-5 (2a–2d)** with Hammett plots using a UV-visible spectrophotometer (Figure 9). *p*-Nitroaniline was used as basic indicator [I] with $pK_a = 0.99$ showing maximum absorbance at 380 nm in blank run which lost its absorption intensity with increasing loading of ionic salts on HZSM-5 (Figure 9), and this change was reflected in Hammett acidity values (Table S3). Hammett acidity function H^0 was determined using the following equation:^[47]

$$H^0 = pK(I)_{aq} + \log\left[\frac{[I]}{[IH^+]}\right] \quad (1)$$

The order of acidity for all the hybrid samples can be arranged with reference to the parent ionic salt as:

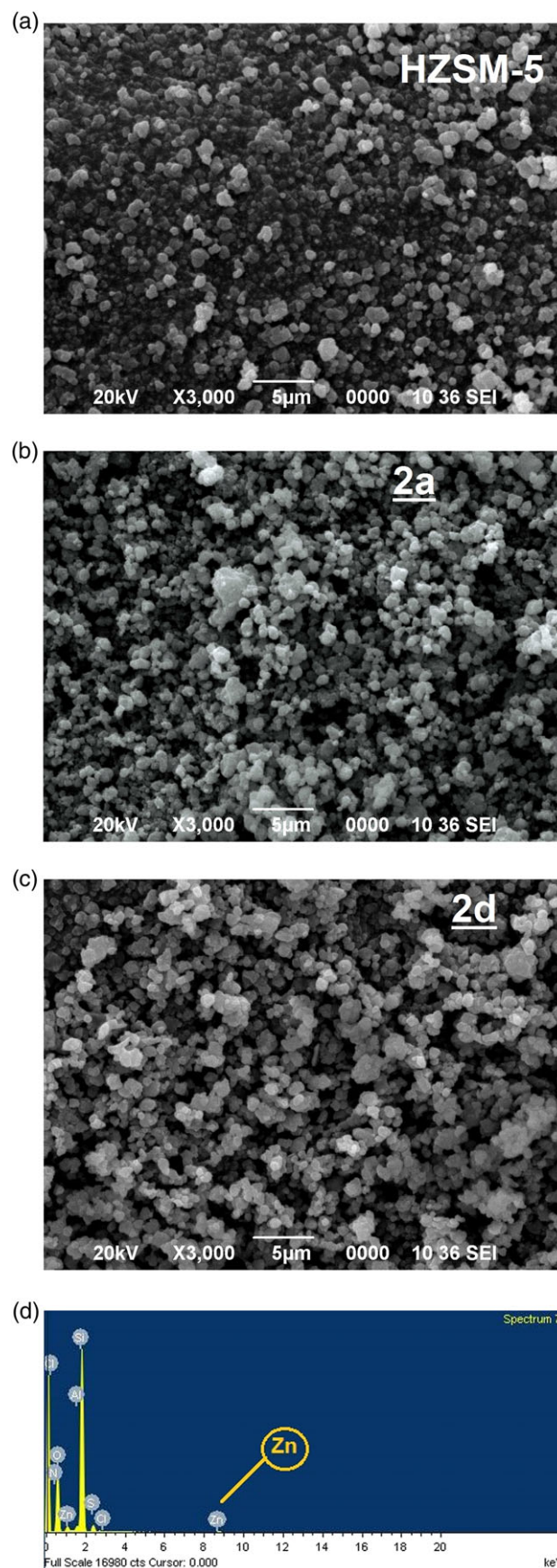


FIGURE 8 SEM images of **2a**, **2d** and HZSM-5, and EDX analysis of **2d**

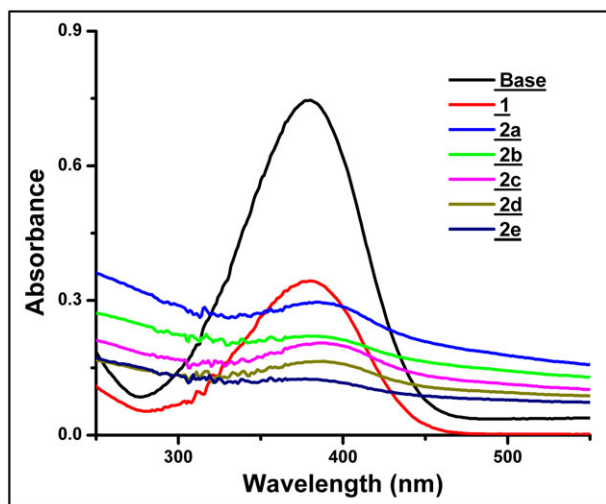


FIGURE 9 Hammett plots of **1**@HZSM-5 in ethanol

2d > **2c** > **2b** > **2a** > **1a**. This increasing trend in Brønsted acidity towards the highest loaded sample may be reasoned in terms of acidic ionic salt-mediated re-alumination of EFAL in HZSM-5 which increased the acidic sites in composites, which was also previously explained in the case of —OH band in absorption spectra^[48] (Figure 3).

3.7 | Lewis acidity determination

The presence of Lewis acidic sites in the synthesized materials (**2a–2e**) was determined using pyridine as probe molecule. FT-IR analysis was conducted, mixing pyridine with **1**@ HZSM-5 (1:3) for all samples. Neat pyridine displays a characteristic band at 1437 cm^{-1} which was shifted to higher wavenumbers in the case of Lewis acidic materials (1440 cm^{-1}) along with shoulder broadening at $1450\text{--}1455\text{ cm}^{-1}$ (Figure 10). This can be reasoned as the Lewis acidity of materials arising from the presence of ZnCl_4^{2-} anion in the ionic salt. Also, the new absorption peak at 1538 cm^{-1} may be explained in terms of the interaction between chlorometallate and pyridine to form pyridinium ion. However, for **2a** and **2b** this peak did not appear. This may be due to the minimal loading of ionic salt on HZSM-5 which was not sufficient to express the formation of pyridinium ion in FT-IR spectra.^[49] It was obvious that the highest loaded sample showed significant Lewis acidity.

3.8 | UV-visible diffuse reflectance spectra

The UV-visible diffuse reflectance spectra of the loaded materials with respect to HZSM-5 were recorded to examine the effect of the loading amount of ionic salt

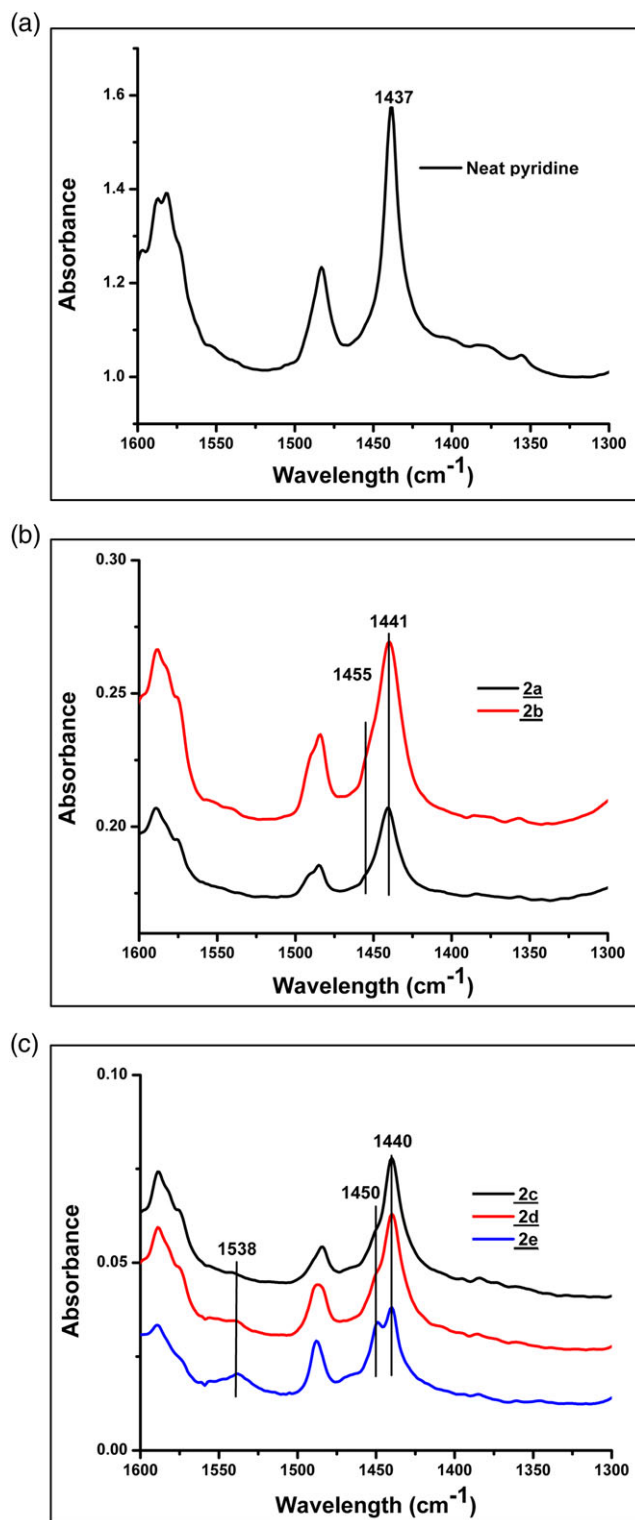


FIGURE 10 FT-IR analysis of Lewis acidity of **1**@HZSM-5 using pyridine

(Figure 11). All the spectra clearly indicate the existence of characteristic constituents of chlorometallate moiety in HZSM-5. Weak absorptions at 260 and 319 nm can be correlated with the intra-ligand charge transfer transitions of the loaded ionic salt **1** at 222 and 340 nm.^[19]

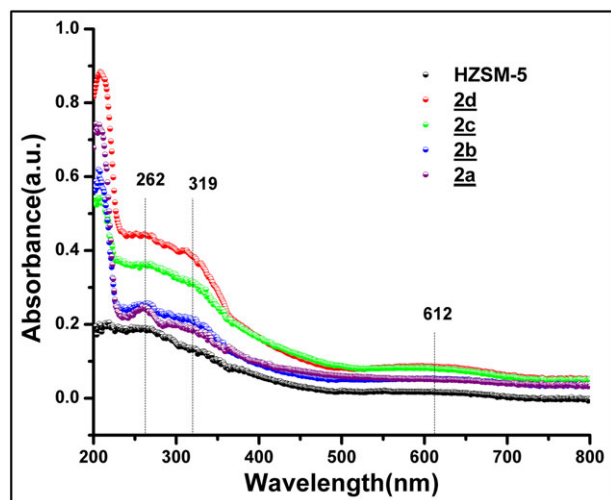


FIGURE 11 UV-visible diffuse reflectance spectra of 1@HZSM-5 (2a–2e) with respect to HZSM-5

3.9 | BET analysis

According to the IUPAC classification, Figure 12a shows characteristics of combined type I and type IV isotherms with type H4 hysteresis loops which indicate the formation of a hierarchical porous system containing both micropores and mesopores. Capillary condensation in inter-/intra-crystalline mesopore void spaces present in the initially de-aluminated HZSM-5 and hybrid materials can be assumed in the region $0.4 < P/P_0 < 0.95$.^[50–52] Figure 12b portrays the Barrett–Joyner–Halenda (BJH) pore size distribution plot of the parent HZSM-5 and 2d (17% loading) using only the adsorption branch of the isotherm. The mean size of the micropores in HZSM-5 and the highest loaded composites was estimated to be about 17.34 Å (1.7 nm).

The t -plots of HZSM-5 and 2d were obtained using the equation given by De Boer:

$$t \text{ (Å)} = [13.99 / (\log(p_0/p) + 0.034)]^{0.5} \quad (2)$$

The positive intercept of the straight line to the y -axis gives the pore volume ($V_{MP} = I \times 0.001547 \text{ cm}^3$). From the slopes of the straight lines derived from t -plots of respective samples in Figure 13, one can determine the external surface areas and mesoporous areas ($A \text{ (m}^2 \text{ g}^{-1}) = \text{slope} \times 15.47$).^[53]

All the results obtained from nitrogen adsorption-desorption isotherms, BJH curves and t -plots are summarized in Table 2. We noticed that a significant decrease in BET surface areas occurred for the highest loaded material as compared to the parent zeolite, which can be justified in terms of clogging or filling of pores by the loaded ionic salt.

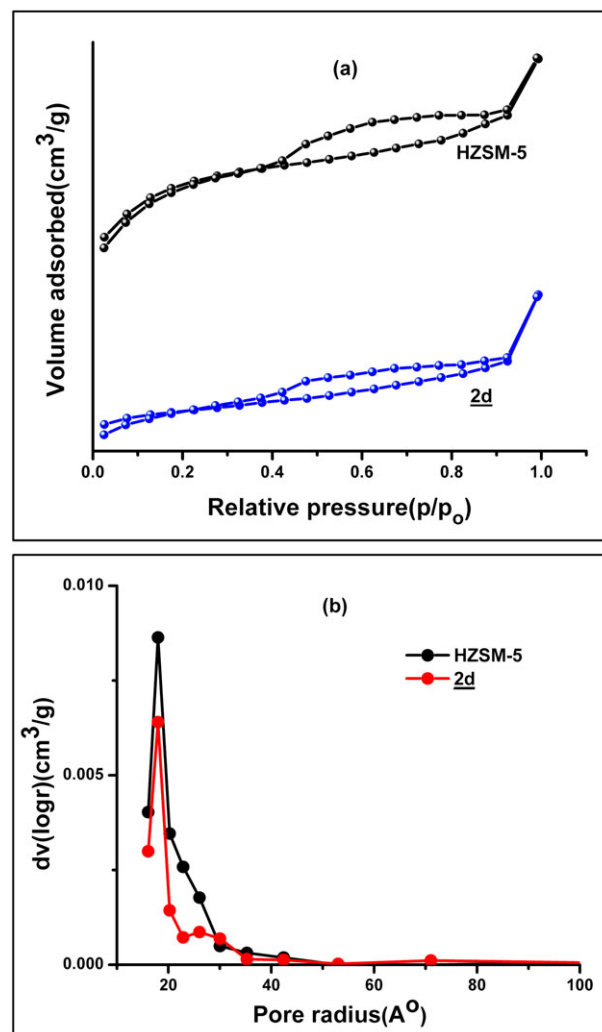


FIGURE 12 (a) Nitrogen isotherms of HZSM-5 and 2d. (b) BJH curves of HZSM-5 and 2d

3.10 | Catalytic activity

The catalytic activity was investigated for all the synthesized materials (2a–2d) in the Fischer indole reaction to synthesize indole derivatives using phenylhydrazine hydrochloride and various ketones or aldehydes (aliphatic/aromatic). The reaction was optimized by using various amounts of acidic catalysts, at various temperatures and also for various solvents. To optimize the reaction given by reaction conditions, a model reaction (Scheme 3) was adopted involving phenylhydrazine hydrochloride (1 mmol) and cyclohexanone (1 mmol) to yield 1,2,3,4-tetrahydrocarbazole (3a) in the presence of various amounts (5, 10 and 15 mg) of catalysts 2a–2d in solvent-free medium at 100°C (Table 3, entries 1–4). The best result was observed for 10 mg of catalyst 2d (Table 3, entry 4). The reaction temperature was

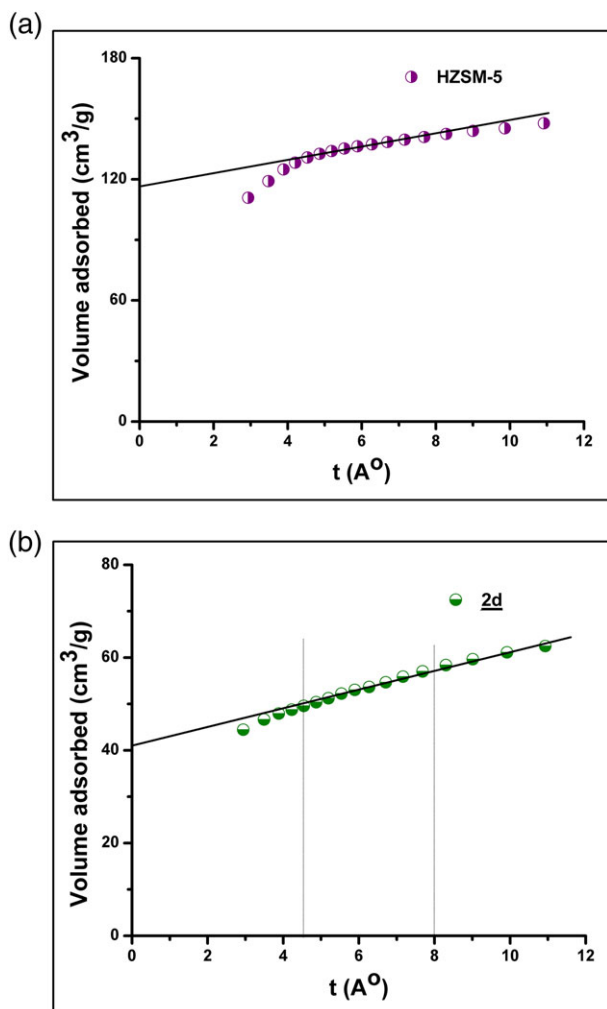
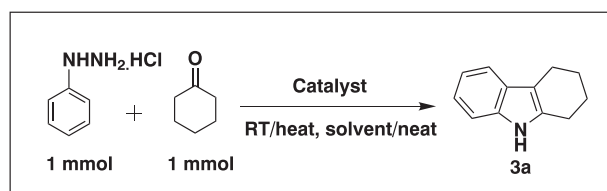
FIGURE 13 *t*-plots of HZSM-5 and **2d**

TABLE 2 Summary of BET analysis

| Material | S_{BET} ($\text{m}^2 \text{g}^{-1}$) ^a | S_{EXT} ($\text{m}^2 \text{g}^{-1}$) ^b | V_{mp} ($\text{cm}^3 \text{g}^{-1}$) ^b | S_{mp} ($\text{m}^2 \text{g}^{-1}$) ^c |
|-----------|---|---|---|--|
| HZSM-5 | 428.77 | 53.34 | 0.178 | 375.43 |
| 2d | 134.94 | 33.97 | 0.064 | 100.97 |

^aSurface area calculated from multipoint BET.^bExternal surface areas and micropore volumes measured by *t*-plot method.^c $S_{\text{mp}} = S_{\text{BET}} - S_{\text{EXT}}$.

SCHEME 3 Synthesis of 1,2,3,4-tetrahydrocarbazole

TABLE 3 Optimization of catalyst amount for synthesis of **3a**

| Entry | Catalyst | Time (h) | | | Yield (%) ^{a,b} | | |
|-------|--|-----------------------------|-------------|-------|--------------------------|-----------|----|
| | | 5 mg | 10 mg | 15 mg | 75 | 80 | 82 |
| 1 | 1 @HZSM-5 = 3% (2a) | 2.75 | 2.5 | 1.75 | 75 | 80 | 82 |
| 2 | 1 @HZSM-5 = 6% (2b) | 2.75 | 2.5 | 1.75 | 80 | 82 | 82 |
| 3 | 1 @HZSM-5 = 9% (2c) | 2 | 1.5 | 1.5 | 85 | 88 | 88 |
| 4 | 1 @HZSM-5 = 17% (2d) | 1.5 | 0.75 | 0.5 | 88 | 95 | 95 |
| 5 | 1 @HZSM-5 = 17% (2d) ^c | 24/1/0.75/0.75 ^c | | | -/75/94/95 ^c | | |
| 6 | 1 @HZSM-5 = 17% (2d) ^d | 0.83/1/1.16 | | | 90/82/90 ^d | | |

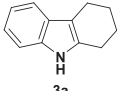
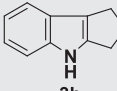
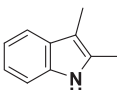
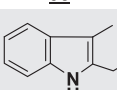
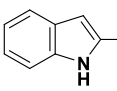
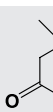
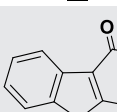
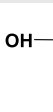
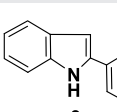
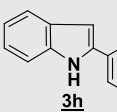
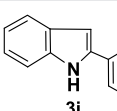
^aIsolated yield.^bReactions of entries 1–4 were conducted at 100°C in neat condition.^cReactions were conducted at room temperature, 60°C, 80°C and 100°C respectively using 10 mg of **2d** in neat condition.^dReactions were performed in CH_2Cl_2 , EtOH and H_2O respectively at temperatures below their boiling points using 10 mg of **2d** as catalyst.TABLE 4 Comparison of catalytic activity of **2d** and previously reported catalysts

| Catalyst | Reaction conditions | Time (h) | Yield of 3a (%) |
|---|----------------------|----------|------------------------|
| 1 @HZSM-5 = 17% (2d) | 10 mg, 100°C | 0.75 | 94 |
| 1 | 10 mg, 100°C | 1.5 | 75 |
| <i>p</i> -Toluenesulfonic acid | 10 mg, 100°C | 8 | 68 |
| ZnCl_2 | 10 mg, 100°C | 6 | 70 |
| H-Y | 1 g, MeOH, 60°C | 18 | 69.3 ^[54] |
| [bmim][HSO ₄] | 70°C in ionic liquid | 1 | 92 ^[55] |
| 50 mol% [cmmim][BF ₄] | 140°C | 2 | 92 ^[56] |
| 20 mol% [bmim][BF ₄] | Reflux in MeOH | 7 | 95 ^[57] |
| 10 mol% [C ₁₀ MIM][Br] | MW, 300 W | 3 min | 58.05 ^[58] |
| 10 mol% [C ₁₀ MIM][Br] + ZnCl_2 | MW, 300 W | 3 min | 94.25 ^[58] |

optimized at 80°C for the same catalyst amount (Table 3, entry 5). The reaction was also conducted in each of CH_2Cl_2 , EtOH and water at temperatures below their boiling points and good results were obtained (Table 3, entry 6).

Based on these optimization results, we extended our investigation with a variety of cyclic, acyclic and aromatic ketone and aliphatic aldehyde compounds with 10 mg of catalyst **2d** at 80–90°C to synthesize substituted

TABLE 5 Substrate scope of indole derivatives using 1@HZSM-5 = 17% (2d) as catalyst

| Entry | Ketone | Time (h) | Product | Yield of product (%) ^a |
|-------|---|----------|--|-----------------------------------|
| 1 |  | 0.75 |  3a | 94 |
| 2 |  | 1 |  3b | 90 |
| 3 |  | 0.83 |  3c | 90 |
| 4 |  | 0.83 |  3d | 90 |
| 5 |  | 0.75 |  3e | 92 |
| 6 |  | 1 |  3f | 82 |
| 7 |  | 1 |  3g | 80 |
| 8 |  | 0.75 |  3h | 88 |
| 9 |  | 0.75 |  3i | 85 |
| 10 | CH ₃ CH ₂ CHO | 2 | — | Complex mixture |
| 11 |  | 2 | — | Complex mixture |

^aIsolated yield.

indole derivatives (Table 4). The reaction involving ketones gave excellent performance in terms of product yield, easy isolation and minimal side product. But in the case of aliphatic aldehydes, namely propionaldehyde and isobutyraldehyde, we obtained complex mixture of products which can be accounted for by acid-catalysed self-condensation of aldehydes containing acidic α -hydrogen with respect to electron-deficient aldehyde group (Table 4, entries 10 and 11). A few data are presented in Table 5 for comparison of the percentage yields of model product 3a for the present catalyst and previously reported ones^[54–58].

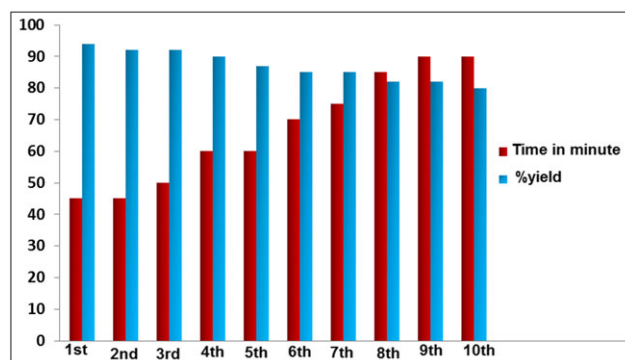


FIGURE 14 Recyclability profile of 2d

3.11 | Reaction mechanism

A plausible reaction mechanism may be expected from simultaneous interactions of both the Brønsted–Lewis acidic sites of the supported catalyst with C=O and also with —NHNH₂ groups through hydrogen bonding as depicted in Scheme S1 (supporting information).

3.12 | Recyclability study

Catalyst recyclability was investigated using the reaction shown in Scheme 3. The model reaction was carried out with 5 mmol of substrates using 50 mg of **2d** as a solid acidic catalyst under standard reaction conditions. After completion of the reaction as monitored by TLC, the reaction mixture was dissolved in DCM whereas the catalyst was insoluble in the same. Decantation of the organic extract separated the solid catalyst from the reaction mixture. Reactivation of the spent catalyst was done after washing two to three times with absolute ethanol and then dried in a vacuum oven at 100°C for 1 h. The dried catalyst was reused and recycled for nine more cycles (Figure 14). ICP-OES and PXRD analyses were performed with the reused catalyst (Table S4 and Figure S1 of supporting information). The ICP-OES results showed slight leaching of metal content in every consecutive cycle which may be accounted for by *in situ* formation of base from the ionic salts and thus causing desilication of the HZSM-5 support after repeated ethanol washing and drying at 100°C during work-up. This type of deactivation process limits the reactivation of spent catalyst using additional ionic salts.

4 | CONCLUSIONS

In this study, we have synthesized and characterized 1@HZSM-5 materials and investigated their catalytic efficiency as dual-acidic catalysts in the Fischer indole reaction of phenylhydrazine hydrochloride with aliphatic/aromatic ketones. These heterogeneous materials with significant surface area and excellent thermal stability are found to be potential candidates for acid-catalysed synthesis of indole derivatives. Impressive Hammett acidity values along with Lewis acidity imparted by ZnCl₄²⁻ play a key role in catalysis. Apart from this, HZSM-5 as a support offers advantages to the materials by limiting the hygroscopic nature of the ionic salt and thus enhancing their stability as excellent heterogeneous catalysts. In comparison with conventional acids and other acidic catalysts the dual-acidic hybrid solids can be considered as better alternatives for acid catalysis in organic synthesis. The excellent performance of

these catalysts lies in the possession of all the properties of HZSM-5 similar to heterogeneous catalysts which bring selectivity to products without formation of many unwanted side products followed by simple isolation and easy recyclability. Also, the dual-acidic character imparted by Lewis acid ZnCl₄⁻ and Brønsted acid group —SO₃H contributes to the good catalytic performance. Thus, this work provides an easy and beneficial route towards heterogeneous catalysis.

ACKNOWLEDGEMENTS

The authors are grateful to Sophisticated Analytical Instrumentation Centre, Tezpur University, for analyses of various samples and SERB-DST, India for funding (research grant no. EMR/2016/002108) to R.B.

ORCID

Susmita Saikia  <http://orcid.org/0000-0003-1276-7025>
 Krishna Puri  <http://orcid.org/0000-0003-1824-556X>
 Ruli Borah  <https://orcid.org/0000-0001-5362-398X>

REFERENCES

- [1] C. Falamaki, M. Edrissi, M. Sohrabi, *Zeolites* **1997**, *19*, 2.
- [2] R. J. Argauer, G. R. Landolt, US Patent 3,702,886 (1972); G. T. Kokotailo, S. L. Lawton, D. H. Olson, W. M. Meier, *Nature* **1978**, *272*, 437.
- [3] S. Sang, F. Chang, Z. Liu, C. He, Y. He, L. Xu, *Catal. Today* **2004**, *93*, 729.
- [4] P. Munnik, P. E. de Jongh, K. P. de Jong, *Chem. Rev.* **2015**, *115*, 6687.
- [5] R. J. White, R. Luque, V. L. Budarin, J. H. Clark, D. J. Macquarrie, *Chem. Soc. Rev.* **2009**, *38*, 481.
- [6] Q. L. Zhu, Q. Xu, *Chem* **2016**, *1*, 220.
- [7] B. C. Gates, *Chem. Rev.* **1995**, *95*, 511.
- [8] J. Liang, Z. Liang, R. Zou, Y. Zhao, *Adv. Mater.* **2017**, *29*, 1701139.
- [9] M. J. Jin, A. Taher, H. J. Kang, M. Choi, R. Ryoo, *Green Chem.* **2009**, *11*, 309.
- [10] J. Guzman, B. C. Gates, *Dalton Trans.* **2003**, 3303.
- [11] A. J. Cruz-Cabeza, D. Esquivel, C. Jiménez-Sanchidrián, F. J. Romero-Salguero, *Materials* **2012**, *5*, 121.
- [12] J. S. D. Oliveira, M. A. Mazutti, E. A. Urquieta-González, E. L. Foletto, S. L. Jahn, *Mater. Res.* **2016**, *19*, 1399.
- [13] A. Kristiani, S. Sudiarmanto, F. Aulia, L.N. Hidayati, H. Abimanyu, In *MATEC Web of Conferences EDP Sciences.* **2017**, *101*, 01001.
- [14] K. Arya, D. S. Rawat, H. Sasai, *Green Chem.* **2012**, *14*, 1956.
- [15] M. Shirani, A. Semnani, S. Habibollahi, H. Haddadi, M. Narimani, *J. Porous Mater.* **2016**, *23*, 701.

- [16] P. Gogoi, A. K. Dutta, R. Borah, *Catal. Lett.* **2017**, *147*, 674.
- [17] J. Estager, A. A. Oliferenko, K. R. Seddon, M. Swadźba-Kwaśny, *Dalton Trans.* **2010**, *39*, 11375.
- [18] R. L. Vekariya, *J. Mol. Liq.* **2017**, *227*, 44.
- [19] S. Saikia, P. Gogoi, A. K. Dutta, P. Sarma, R. Borah, *J. Mol. Catal. A* **2016**, *416*, 63.
- [20] C. P. Mehnert, *Chem. Eur. J.* **2005**, *11*, 50.
- [21] P. Gogoi, A. K. Dutta, S. Saikia, R. Borah, *Appl. Catal. A* **2016**, *523*, 321.
- [22] D. L. Hughes, *Org. Prep. Proced. Int.* **1993**, *25*, 607.
- [23] E. Yasui, M. Wada, N. Takamura, *Tetrahedron Lett.* **2006**, *47*, 743.
- [24] K. Alex, A. Tillack, N. Schwarz, M. Beller, *Angew. Chem. Int. Ed.* **2008**, *47*, 2304.
- [25] A. Dhakshinamoorthy, K. Pitchumani, *Appl. Catal. A* **2005**, *292*, 305.
- [26] M. Platon, R. Amardeil, L. Djakovitch, J. C. Hierro, *Chem. Soc. Rev.* **2012**, *41*, 3929.
- [27] W. C. Neuhaus, I. J. Bakanas, J. R. Lizza, C. T. Boon, G. Moura-Letts, *Green Chem. Lett. Rev.* **2016**, *9*, 39.
- [28] T. O. ShrungheshKumar, K. M. Mahadevan, *Org. Commun.* **2013**, *6*, 31.
- [29] I. L. Librando, E. C. Creencia, *Procedia Chem.* **2015**, *16*, 299.
- [30] V. Sharma, P. Kumar, D. Pathak, *J. Heterocycl. Chem.* **2010**, *47*, 491.
- [31] N. K. Kaushik, N. Kaushik, P. Attri, N. Kumar, C. H. Kim, A. K. Verma, E. H. Choi, *Molecules* **2013**, *18*, 6620.
- [32] G. L. Rebeiro, B. M. Khadilkar, *Synthesis* **2001**, 370.
- [33] R. C. Morales, V. Tambyrajah, P. R. Jenkins, D. L. Davies, A. P. Abbott, *Chem. Commun.* **2004**, 158.
- [34] D. Q. Xu, J. Wu, S. P. Luo, J. X. Zhang, J. Y. Wu, X. H. Du, Z. Y. Xu, *Green Chem.* **2009**, *11*, 1239.
- [35] B. L. Li, D. Q. Xu, A. G. Zhong, *J. Fluorine Chem.* **2012**, *144*, 45.
- [36] L. L. Tao, J. Jiang, Y. C. Pan, X. Yang, B. L. Li, *Adv. Mater. Res.* **2013**, *661*, 150.
- [37] Y. L. Hu, D. Fang, D. S. Li, *Catal. Lett.* **2016**, *146*, 968.
- [38] W. Fan, R. Li, J. Ma, B. Fan, J. Cao, *Micropor. Mater.* **1995**, *4*, 301.
- [39] P. A. Jacobs, H. K. Beyer, J. Valyon, *Zeolites* **1981**, *1*, 161.
- [40] J. C. Jansen, F. J. Van der Gaag, H. V. Beckum, *Zeolites* **1984**, *4*, 369.
- [41] G. Coudurier, C. Naccache, J. C. Vedrine, *J. Chem. Soc. Chem. Commun.* **1982**, *24*, 1413.
- [42] K. Yamagishi, S. Namba, T. Yashima, *J. Phys. Chem.* **1991**, *95*, 872.
- [43] Y. Fan, X. Bao, X. Lin, G. Shi, H. Liu, *J. Phys. Chem. B* **2006**, *110*, 15411.
- [44] Y. Zhang, Y. Zhou, L. Huang, M. Xue, S. Zhang, *Ind. Eng. Chem. Res.* **2011**, *50*, 7896.
- [45] M. Khatamiana, M. Irania, *J. Iran. Chem. Soc.* **2009**, *6*, 187.
- [46] F. Fan, K. Sun, Z. Feng, H. Xia, B. Han, Y. Lian, P. Ying, C. Li, *Chem. Eur. J.* **2009**, *15*, 3268.
- [47] C. Thomazeau, H. Olivier-Bourbigou, L. Magna, S. Luts, B. Gilbert, *J. Am. Chem. Soc.* **2003**, *125*, 5264.
- [48] L. Shirazi, E. Jamshidi, M. R. Ghasemi, *Cryst. Res. Technol.* **2008**, *43*, 1300.
- [49] Y. L. Yang, Y. Kou, *Chem. Commun.* **2004**, 226.
- [50] M. Thommes, K. Kaneko, A. V. Neimark, J. P. Olivier, F. Rodriguez-Reinoso, J. Rouquerol, K. S. Sing, *Pure Appl. Chem.* **2015**, *87*, 1051.
- [51] L. Vafi, R. Karimzadeh, *Chin. J. Catal.* **2016**, *37*, 628.
- [52] R. Kore, R. Srivastava, B. Satpati, *Chem. Eur. J.* **2014**, *20*, 1.
- [53] P. Voogd, J. J. F. Scholten, H. Van Bekkum, *Colloids Surf.* **1991**, *55*, 163.
- [54] D. Bhattacharya, D. W. Gammon, E. Van Steen, *Catal. Lett.* **1999**, *61*, 93.
- [55] D. Q. Xu, W. L. Yang, S. P. Luo, B. T. Wang, J. Wu, Z. Y. Xu, *Eur. J. Org. Chem.* **2007**, *6*, 1007.
- [56] F. P. Yi, H. Y. Sun, X. H. Pan, Y. Xu, J. Z. Li, *Chin. Chem. Lett.* **2009**, *20*, 275.
- [57] T. O. S. Kumar, K. M. Mahadevan, *Org. Commun.* **2013**, *6*, 31.
- [58] I. L. Librando, E. C. Creencia, *Procedia Chem.* **2015**, *16*, 299.

SUPPORTING INFORMATION

Additional supporting information may be found online in the Supporting Information section at the end of the article.

How to cite this article: Saikia S, Puri K, Borah R. Supported dual-acidic 1,3-disulfoimidazolium chlorozincate@HZSM-5 as a promising heterogeneous catalyst for synthesis of indole derivatives. *Appl Organometal Chem.* 2019;e4672. <https://doi.org/10.1002/aoc.4672>